Effects of Forest Connectivity on the Spatial Synchrony of Outbreaks of a Forest Defoliating Insect

Catherine O'Connor Porter
Hopewell, New Jersey

BS, Brown University, 2020

A Thesis presented to the Graduate Faculty of
the University of Virginia in Candidacy for the Degree of
Master of Science

Department of Environmental Science

University of Virginia
May, 2023

Kyle Haynes
Xi Yang
Stephan De Wekker

Abstract

Synchronous fluctuations in the densities or population growth of spatially disjunct populations are ubiquitous. The factors responsible for driving this spatial synchrony have long spurred speculation. Traditionally, spatial synchrony in populations is thought to be caused by synchrony in environmental factors (the "Moran effect"), trophic interactions with another species that exhibits synchronous population fluctuations, or dispersal among populations. Since the direct effects of dispersal are difficult to quantify, I investigated the relationship between forest connectivity and the spatial synchrony of outbreaks of the forest defoliating insect *Lymantria dispar*. Forest connectivity was modeled using circuit theory. Effects of forest connectivity were assessed both across different sampling scales and over different distances (10km, 25km, 50km, and 100km). I found significant positive effects of the connectivity of *L. dispar* host trees as well as significant positive and negative effects of all tree species combined on spatial synchrony across the different scales of analysis. This suggests that dispersal is a significant driver of the spatial synchrony in this system. This approach exploring the relationship between spatial synchrony and forest connectivity assessed through circuit theory can be used in future studies as a framework for investigating possible differences in the effects of dispersal on synchrony across spatial scales.

1. Introduction

Spatial synchrony refers to the phenomenon whereby the dynamics of populations separated by space are correlated through time (Liebhold *et al*. 2004). This phenomenon has been observed in a variety of ecological phenomenon across virtually all taxa. Spatial synchrony has important implications for the conservation of species as the likelihood of global metapopulation persistence is diminished if local populations synchronously fluctuate to low abundances (Brown & Kodric-Brown 1977; Heino *et al.* 1997; Vogwill *et al.* 2009). Spatial synchrony is also an important consideration in pest management, as only populations that fluctuate synchronously over large areas can exhibit regional-scale outbreaks causing substantial impacts (Liebhold *et al.* 2012).

Dispersal among spatially disjunct populations is one of three factors know to be capable of driving population spatial synchrony (Ranta *et al.* 1995), the others being spatial synchrony in environmental fluctuations (Moran 1953, Ranta *et al*. 1997) and species interactions between a focal species and another species that displays spatial synchrony (Haynes *et al*. 2009). Population synchronization can be driven by the dispersal of the focal species itself (Hansson 1991; Ims & Yoccoz 1996; Steen *et al.* 1996) or by dispersal of the focal species' natural enemies (Ydenberg 1987; Ims & Steen 1990; Hanski & Woiwod 1993; Bjornstad *et al.* 1999). For example, in theory, movement of nomadic avian predators will increase the spatial synchrony of populations of the rodent prey (Ims & Steen 1990).

For most species, the mechanisms leading to spatially synchronous dynamics are unknown. It is difficult to discern these drivers because, for example, the creation of reliable long-term datasets over wide geographic areas is time and resource intensive, empirical dispersal data are difficult to collect at any scale, and traditional statistical methods for analyzing spatial synchrony have not provided practical ways to weigh the evidence for and against different mechanisms (Liebhold & Kamata 2000; Peltonen *et al.* 2002). Furthermore, there may be multiple drivers of synchrony within a given study system.

Different drivers of synchrony have often been assumed to influence population synchrony over different spatial scales, however few studies have examined this possibility. For example, based on observations that the outbreaks of forest insect pest species tended to exhibit spatial synchrony over large distances (hundreds of km), Peltonen *et al.* (2002) argued that the synchrony of these outbreaks was likely primarily a result of broad-scale synchrony in environmental fluctuations. Still, the authors found that population synchrony declines with distance more rapidly than does the synchrony of temperature and precipitation. For the forest defoliating moth *Lymantria dispar*, Peltonen *et al.* (2002) ascribed the discrepancy in rates of distance decay in the strength of synchrony to local heterogeneity in population dynamics. Although it is theoretically possible for short-distance dispersal to synchronize population fluctuations over large distances (Fox *et al.* 2011), dispersal may promote population spatial synchrony over shorter distances than does synchrony in environmental fluctuations (Steen *et al.* 1996; Bjornstad *et al.* 1999; Ims & Andreassen 2000; Stenseth *et al.* 1999).

The effects of dispersal on population spatial synchrony have largely been studied only theoretically (Bjornstad & Bolker 2000; Ranta *et al.* 1998; Lande *et al.* 1999) or in laboratory populations (Laan & Fox 2019; Fox *et al.* 2013). Its importance in field populations is less well understood. It is difficult to directly quantify the frequency distribution of dispersal distances (or dispersal kernel) since recapture rates may be low (Nathan 2001; Bullock *et al.* 2006; Rieux *et al.* 2014; Rogers *et al.* 2019). This is especially true for long-distance dispersal, since the total necessary sample area will increase exponentially with dispersal distance.

In addition to recent evidence from population genetic sampling (Larroque *et al.* 2019; Larroque *et al.* 2020; Legault *et al.* 2021), some of the clearest evidence of effects of dispersal on the spatial synchrony of populations in nature may stem from studies examining relationships between habitat connectivity and population spatial synchrony because of the linkage between habitat connectivity and dispersal rates. The strength of population spatial synchrony is typically expected to increase with the degree of habitat connectivity given higher rates of dispersal among subpopulations (Bellamy *et al.* 2003). Consistent with this expectation, the synchrony of woodland birds in the United Kingdom was found to be stronger across areas with more woodlands (Bellamy *et al.* 2003). Another study found that pairwise distance through woodland-edges was a better predictor of the population synchrony of Ringlet butterflies (which use woodland-edges as a primary habitat) than was Euclidean distance (Powney *et al.* 2012). For plankton inhabiting a reservoir, Anderson *et al.* (2017) found that predictions of rates of dispersal among locations (i.e., functional connectivity) based on water currents alone explained, on average, 26% of the variation in spatial synchrony across different taxa.

The tremendous spatial and temporal extent of the record on defoliation of forests by the spongy moth *Lymantria dispar* in North America makes this an ideal study organism for understanding the mechanisms driving population spatial synchrony. The proportion of land area defoliated by *L. dispar* can be used as a proxy for population density (Peltonen *et al.* 2002; Johnson *et al.* 2006). Spatial synchrony in *L. dispar* defoliation occurs over distances up to 1200km (Haynes *et al.* 2009). Recent studies have explored the causes of spatial synchrony in *L. dispar* outbreaks by leveraging geographic variation in the synchrony of *L. dispar* defoliation. Studies have identified spatial synchrony in precipitation as a primary driver of the spatial synchrony of *L. dispar* outbreaks (Haynes *et al.* 2013, Haynes *et al.* 2018). However, these studies examined spatial synchrony of *L. dispar* outbreaks only over large distances. For example, Haynes *et al.*'s (2013) analysis was based on data consisting of the proportion of forest defoliated in 64 × 64 km cells. Consequently, potential impacts of dispersal on local synchrony over distances < 64 km were ignored.

I investigated the role of dispersal as a driver of the spatial synchrony of *L. dispar*. Because *L. dispar* and its chief predator, the white-footed mouse *Peromyscus leucopus*, are forest-dwelling organisms, I hypothesized that increasing forest connectivity positively affects the spatial synchrony of *L. dispar* outbreaks. The white-footed mouse may disperse more easily through large continuous tracts of forest than through unforested habitat types given that the mouse prefers forest interior habitat over forest edges (Morris & Diffendorfer 2002). Increased

dispersal by *L. dispar* predators may in turn increase the spatial synchrony of *L. dispar* populations. Based on the expected effects of forest connectivity on the dispersal of *L. dispar* and its small mammal predators, I hypothesized that the synchrony of *L. dispar* outbreaks increases with forest connectivity.

3. Methods

3.1 Study system

Since its introduction to the United States in the 1860s, *L. dispar* continues to be a damaging forest pest in eastern North America, defoliating vast tracts of forest during outbreaks (Twery 1990, Morin & Liebhold 2016). *Lymantria dispar* is highly polyphagous, feeding on > 200 tree species in North America, but displays strong preferences for certain host species over others (Liebhold *et al.* 1995). In North America, the dominant preferred host trees of *L. dispar* are oaks, birches, and poplars (Haynes *et al.* 2022).

Adult females of *L. dispar* in North America are incapable of flight (Elkinton & Liebhold 1990). 'Ballooning' of first instar larvae is *L. dispar*'s main natural method of dispersal (Elkinton & Liebhold 1990). Ballooning describes the behavior in which first instar larvae climb to the upper canopy, from where they spin down on silk strands and can be transported by winds. The dispersal distances of ballooning *L. dispar* larvae rarely exceed 200 m (Mason & McManus 1981). Longer-distance dispersal occurs via occasional accidental human transport (typically of egg masses) (McFadden & McManus 1991; Tobin & Blackburn 2014). Because such long-distance anthropogenic dispersal is rare, it probably has little influence linking established populations though it can be of considerable importance in facilitating invasion of new regions (Liebhold & McManus 1991).

The predominant natural enemies of *L. dispar* differ in their dispersal capabilities, which may affect their relative impacts on the spatial synchrony of *L. dispar* outbreaks. These natural enemies include the fungal pathogen *Entomophoga maimaiga*, the *Lymantria dispar* nuclear polyhedrosis virus (*Ld*NPV), small-mammal predators, and parasitoids (Liebhold *et al.* 2004). The viral pathogen cannot disperse on its own, but some parasitoids of *L. dispar* are known to be able to vector *Ld*NPV (Reardon & Podgwaite 1976). Little is known about the dispersal ability of the parasitoids of *L. dispar*, but tachinid parasitoids of *L. dispar* may disperse on the scale of several kilometers (Munro 1998). The lifetime dispersal distance of the chief predator of *L. dispar*, the white-footed mouse, has been reported to be as high as 14km (Maier 2002), but is typically < 1 km (Howard 1949; Krohne *et al.* 1984). *Entomophoga maimaiga* conidial spores, as opposed to resting spores which have effectively no dispersal ability, are known to be carried by wind across distances up to 100km (Weseloh 2003) and recent work shows that conidia disperse up to 70 km from outbreak populations (Bittner et al., 2017, Elkinton et al. 2019). The dispersal ability of the conidia of *E. maimaiga* far exceeds any of *L. dispar's* other natural enemies.

3.2 Forest connectivity

To examine the effects of forest connectivity on the spatial synchrony of *L. dispar* outbreaks, I examined geographic variation in the strength of the synchrony of *L. dispar* defoliation from 1990 to 2018 in areas of the northeastern United States that were invaded by 1990 (based on the designation of counties in historical USDA *L. dispar* domestic quarantine regulations, U.S. Code of Federal Regulations, Title 7, Chapter III, Section 301.45-4). Michigan was excluded because it is not contiguous with the rest of the study area. Annual aerial surveys of *L. dispar* defoliation compiled by the USDA Forest Service (USFS) were used to generate GIS raster layers of 2 × 2km cells (Liebhold *et al.* 1997). From these spatiotemporal defoliation data, geographic variation in the strength of local synchrony in defoliation was calculated using the non-centered local indicator of spatial association (ncLISA; Gouveia *et al.* 2016). This procedure was implemented using the function 'lisa.nc' from the R package 'ncf' (Bjørnstad 2020). Using the ncLISA procedure, the strength of synchrony in defoliation for each focal cell was estimated as the mean of the pairwise measures of synchrony (Pearson correlation) in defoliation between the focal cell and all surrounding cells within a neighborhood of specified size (i.e., within a radius of 10km, 25km, 50km, or 100km). Different neighborhood sizes were used to examine whether the effects of dispersal on synchrony could be captured at different spatial scales, potentially revealing which dispersing agents are largely responsible for driving synchrony.

To distinguish between the importance of the connectivity of forest with high densities of preferred host trees and the connectivity of forest with high densities of trees irrespective of species composition, forest spatial structure was assessed based on maps of (1) basal area (m^2/km^2) of preferred *L. dispar* hosts and (2) basal area of all tree species combined, respectively. These data were obtained by extracting 250 × 250 m resolution data on the basal areas of tree species from Individual Tree Species Parameter Maps (ITSPM; Wilson *et al.* 2013) and aggregating it into the 2 × 2 km cells of the defoliation data. These ITSPM data are derived from extensive field surveys in forest plots across the U.S. carried out by the Forest Inventory & Analysis (FIA) program combined with remotely sensed phenology data from MODIS imagery to produce the final maps. These data are validated and adjusted according to the presence or absence of tree canopy cover using the National Land-Cover Database (NLCD; Wilson *et al.* 2013). The final 250 m basal area estimates are computed as weighted means that are dependent on the proportion of forest to non-forest area calculated at 30m resolution (Wilson *et al.* 2012). Host basal area was based on summing the basal area of each preferred tree species; designation of a tree species as preferred was based on Liebhold et al. (1995). The defoliation, total tree basal area, and host tree basal area data were each compiled to cell sizes of 2 × 2 km, 4 × 4 km, 8 × 8 km, and 16 × 16 km cells to assess the sensitivity of my findings to sampling scale.

I then produced two maps of forest connectivity for each cell size, one based on the assumption that dispersal rates of *L. dispar* or its small mammal predators through a landscape increase with the basal area of *L. dispar* host trees, and the other that dispersal rates increase with

the basal area of all tree species combined. The maps of connectivity were generated using the program Omniscape (Landau *et al.* 2021). Omniscape employs circuit theory, which is based on Ohm's Law, where voltage (referred to as "source strength") and resistance (or its inverse, conductance) are used to calculate current. In an ecological context, conductance can be thought of as the permeability of an area to the movement of organisms and current is analogous to the expected net movement probability of organisms (McRae et al. 2008). The source strength of a cell represents the contribution of that cell to the organism's population growth (Landau *et al.* 2021; Anantharaman *et al.* 2019; McRae *et al.* 2008). Using a moving window approach, Omniscape calculates cumulative current flow to each focal cell from all cells within a chosen focal radius. This cumulative current flow is analogous to the cumulative net movement of organisms to the focal cell. This results in a measure of omni-directional connectivity that is suitable for landscapes with mixed surface types (Landau *et al.* 2021). I use normalized cumulative current flow (NCC), which is cumulative current flow divided by flow potential, as a proxy for forest connectivity. Here, the values of conductance and source strength for each cell were either the basal area of all trees or the basal area of *L. dispar* host trees.

To assess the relationships between the spatial synchrony of *L. dispar* outbreaks and the NCC, I employed generalized-least-squares (GLS) regression (Aitken 1936). The GLS regression approach allowed me to account for spatial autocorrelation. Unlike least-squares regression, in GLS regression there is no assumption that model residuals are uncorrelated. I compared GLS models using different functions for describing the spatial decay in the autocorrelation in residuals (Gaussian, exponential, or no spatial structure). I chose the function for the residuals by selecting the GLS model with the lowest AIC value. This analysis was performed with the R package "nlme" (Pinheiro *et al.* 2021). It was reproduced four times at the different raster resolutions (2km, 4km, 8km, and 16km). The response variable in these models was mean synchrony of defoliation between a focal cell and all the cells within its local neighborhood (i.e., within a radius of 10km, 25km, 50km, or 100km). The explanatory variables were the normalized cumulative current flow based on maps of host tree basal area and the basal area of all tree species combined. We also included mean host basal area and mean basal area of all tree species combined within the neighborhood as covariates to partition potential effects of mean basal area from effects arising from the spatial configuration of forest.

4. Results

The basal area of *L. dispar* host trees tended to be highest in the southeastern portion of the study region (corresponding to the Central Appalachian Mountains) (Fig. 1), while basal area of all tree species combined tended to be higher in the northern portion of the map. The maps of forest normalized cumulative current (Fig. 2) corresponded with the maps of basal area (host or all trees), especially as the radius of the neighborhood increased. This is particularly evident in areas like northern New York and ridges of the Appalachian Mountains. The strength of synchrony in defoliation was typically lower around the central regions of the map (the West

Virginia/Maryland border, central Pennsylvania, and Massachusetts), and higher in the far southern and western portions of the map, as well as areas of the northeastern coast (northern Virginia, western Pennsylvania, and Connecticut; Fig. 3). Figures showing maps for all raster and neighborhood sizes not shown can be found in the Appendix.

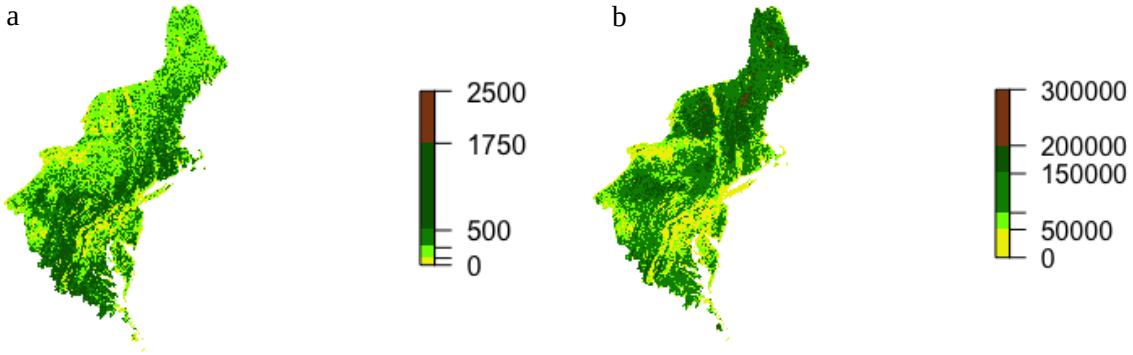

Figure 1. Maps at 2km resolution of basal area (m^2/km^2) of *Lymantria dispar* host trees (a) and basal area of all tree species combined (b), ranging from low (yellow) to high (brown), from the Individual Tree Species Parameter Maps (Wilson *et al.* 2013). The extent of the map is limited to the areas of the U.S. infested with *L. dispar* by 1990 (excluding Michigan).

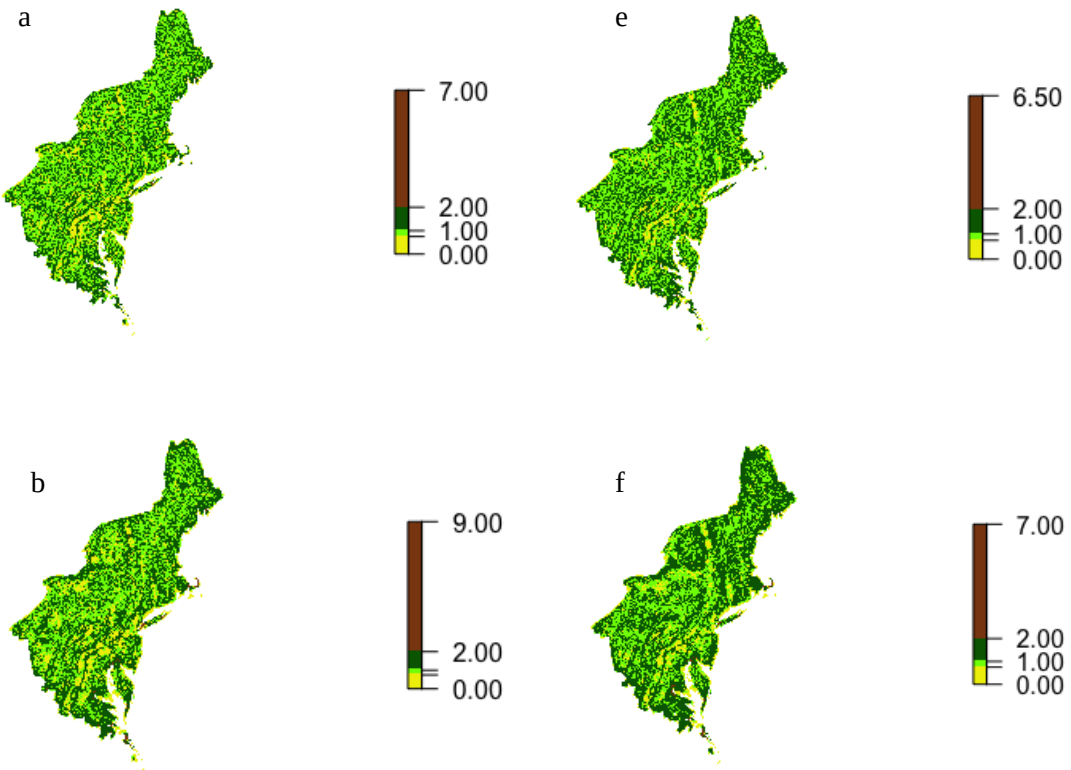

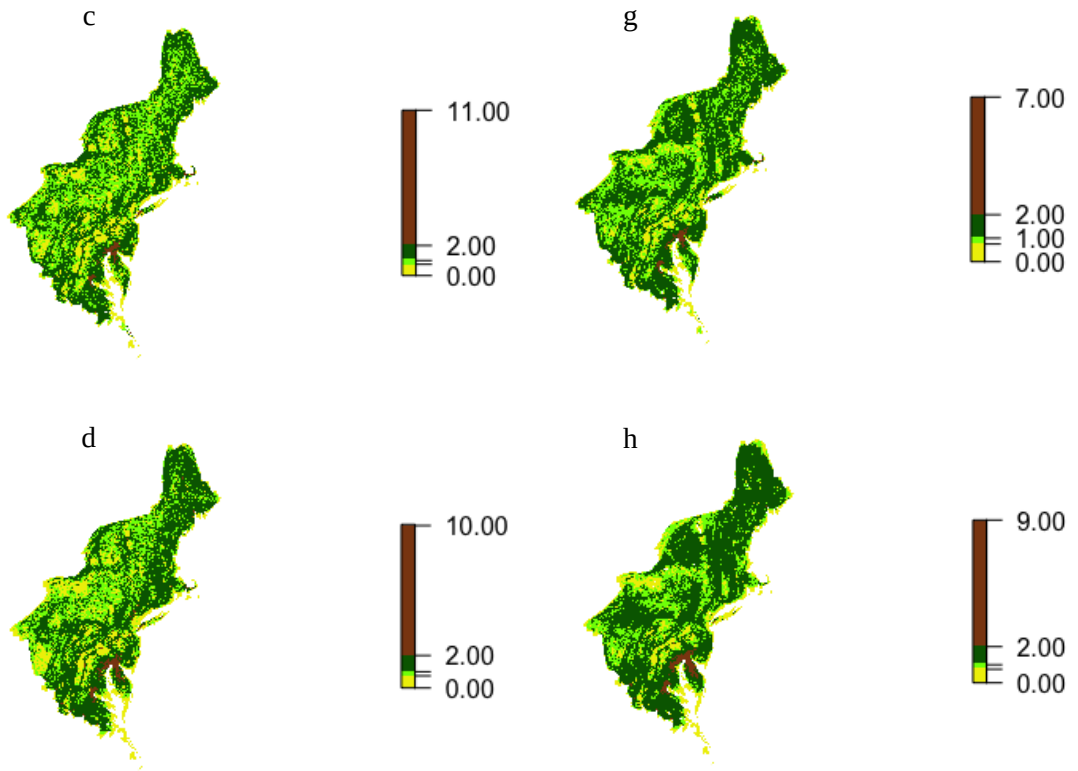

Figure 2. Maps of normalized cumulative current (NCC) where the conductance of 4-km^2 cells was the basal area of *Lymantria dispar* host trees (left column, a-d) or the basal area of all tree species combined (right column, e-h). The NCC flowing to each focal cell from all cells within a neighborhood of a given size (within 10km, 25km, 50km, and 100km respectively) are shown. Values of NCC less than one indicate impeded connectivity, while values > 1 indicate channelized flow.

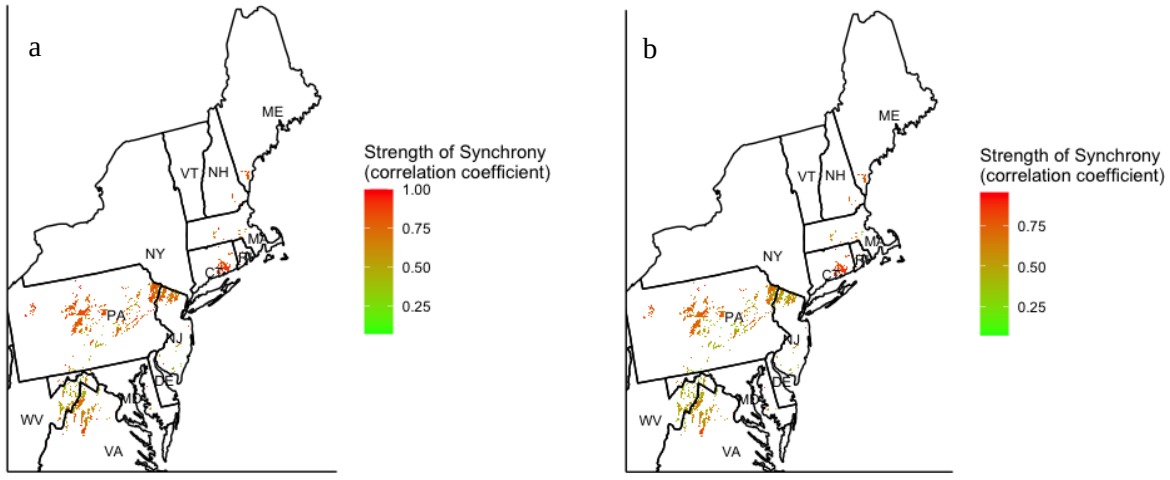

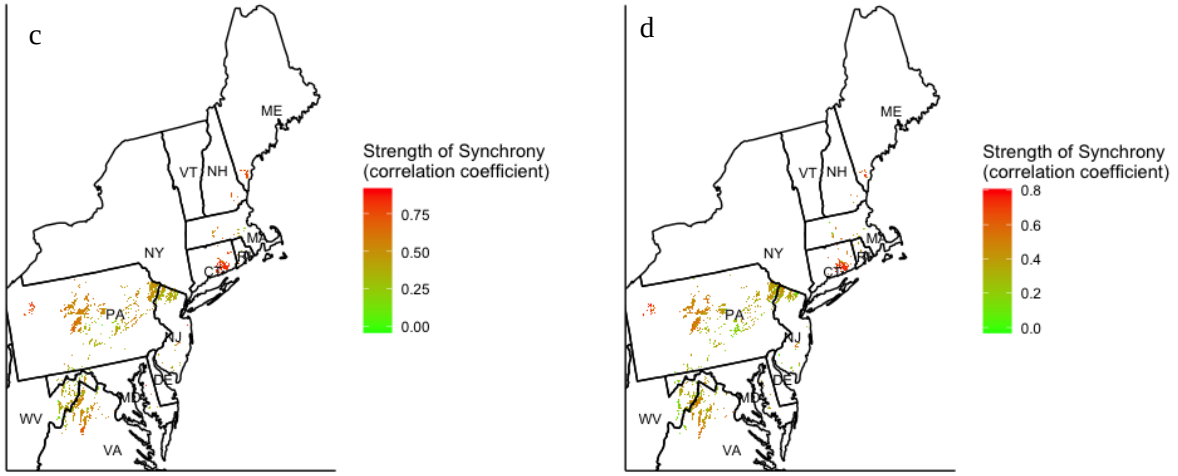

Figure 3. Maps at 2km resolution of strength of synchrony in defoliation by *Lymantria dispar* for all cells with four or more years of defoliation. The strength of local synchrony in defoliation for each of these focal cells was calculated using the non-centered local indicator of spatial association (ncLISA; Gouveia *et al.* 2016) and estimated as the mean of the pairwise measures of synchrony (Pearson correlation) in defoliation between the focal cell and all surrounding cells within a neighborhood of specified size (within a radius of 10 km, 25 km, 50 km, and 100 km respectively, a-d).

There were significant positive effects of NCC of total basal area on the strength of local synchrony in defoliation at the smaller radii sizes and significant negative effects at the larger radii sizes for the 2-km resolution raster (Table 1). At the resolution of 4km, there were significant positive effects of NCC of total basal area at the 10-km and 25-km radii. There were also significant positive effects of mean neighborhood basal area of host tree species and significant negative effects of total tree mean neighborhood basal area at the 10km radius size. There were significant positive effects of NCC of host basal area at the 25-km and 50-km radii for the 8-km resolution raster and at the 100-km radius for the 16-km resolution raster. NCC of total basal area also had significant negative effects at the 100-km radius for the 16-km resolution raster. NCC and mean neighborhood basal area of host basal area always had positive effects when significant, while total tree NCC had both positive and negative significant effects and total tree mean neighborhood basal area always had negative effects where significant.

At all spatial scales, the GLS models which performed the most reliably according to AIC values were those where an exponential function describing the spatial decay in the residuals. The variance inflation factor (VIF) values for all variables were < 10, indicating that multicollinearity of the explanatory variables was not problematic.

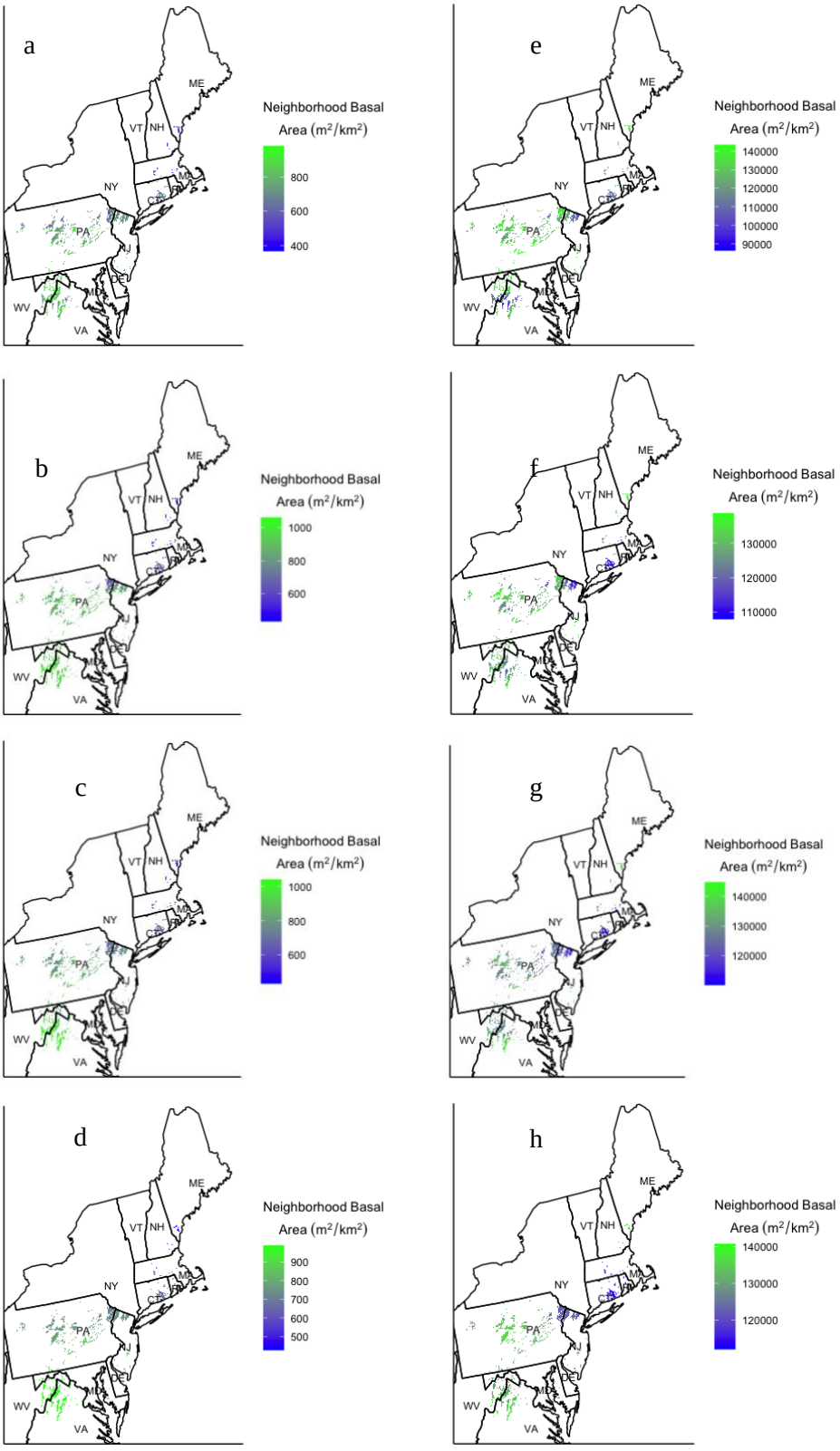

Figure 4. Maps of mean neighborhood basal area of the basal area of *Lymantria dispar* host trees (left column, a-d) or the basal area of all tree species combined (right column, e-h). The means calculated within a neighborhood of a given size (within 10 km, 25 km, 50 km, and 100 km respectively) are shown.

Table 1. Results of the generalized least squares regression on the effects of two measures of normalized cumulative current (NCC) and two measures of tree basal area on the strength of local synchrony of defoliation by *Lymatria dispar*. The analyses were conducted on rasters with 2 × 2km, 4 × 4km, 8 × 8km, and 16 × 16km cells, with mean neighborhood basal area calculated within a radius of each focal cell (10 km, 25 km, 50 km, 100 km). Significant effects ($p < 0.05$) are noted using asterisks.

	2km Raster		**4km Raster**		**8km Raster**		**16km Raster**	
	Coefficient	p-value	Coefficient	p-value	Coefficient	p-value	Coefficient	p-value
10km radius								
Basal area (all tree species)	-0.314	0.072	-0.462	0.030*	0.106	0.407		
Basal area of host trees	0.166	0.0779	0.359	0.040*	0.010	0.930		
NCC of basal area (all tree species)	0.087	< 0.001*	0.130	0.004*	0.035	0.649		
NCC of host tree basal area	0.001	0.899	0.035	0.299	0.116	0.074		
25km radius								
Basal area (all tree species)	-0.073	0.801	0.012	0.963	0.184	0.349	0.184	0.247
Basal area of host trees	0.253	0.079	-0.121	0.555	-0.028	0.876	-0.078	0.578
NCC of basal area (all tree species)	0.044	0.011*	0.068	0.047*	-0.045	0.412	-0.039	0.670
NCC of host tree basal area	-0.008	0.312	0.029	0.238	0.129	0.004*	0.085	0.255
50km radius								
Basal area (all tree species)	0.145	0.505	-0.090	0.795	0.190	0.436	0.194	0.245
Basal area of host trees	0.276	0.044*	0.192	0.557	-0.066	0.768	-0.098	0.471
NCC of basal area (all tree species)	-0.033	0.024*	-0.008	0.778	-0.070	0.120	-0.072	0.228
NCC of host tree basal area	-0.004	0.559	0.018	0.363	0.074	0.027*	0.085	0.055
100km radius								
Basal area (all tree species)	-0.019	0.895	0.2079024	0.4534	0.070	0.699	0.250	0.179
Basal area of host trees	-0.034	0.847	-0.353773	0.2877	-0.047	0.785	-0.206	0.253
NCC of basal area (all tree species)	-0.079	< 0.001*	-0.0359431	0.1078	-0.049	0.129	-0.129	0.009*
NCC of host tree basal area	0.001	0.935	0.0000435	0.9976	0.029	0.192	0.097	0.009*

5. Discussion

Forest connectivity, estimated based on the application of circuit theory to maps of the basal area of all tree species combined or the basal area of *L. dispar* host trees, appeared to have effects on the spatial synchrony of *L. dispar* outbreaks across different spatial scales. Connectivity of *L. dispar* host trees had significant positive effects for the coarser spatial resolutions and over longer distances, whereas the connectivity based on basal area of all tree species had significant positive effects for the finer resolutions and over shorter distances. One mechanism that could explain the positive relationships between connectivity of *L. dispar* host trees and the synchrony of *L. dispar* outbreaks over longer distances is dispersal by the specialist fungal pathogen *E. maimaiga*, which can disperse up to 70km (Bittner *et al.* 2017). The positive relationships between connectivity of all trees and the synchrony of *L. dispar* outbreaks across shorter distances may be driven by the generalist natural enemies of *L. dispar*, including the white-footed mouse and tachinid parasitoids. The distributions of these organisms are not limited to *L. dispar* host trees since *L. dispar* is just one of their prey species. Significant negative effects of the connectivity of all tree basal area are thought to be spurious since there are no known reasons why decreased habitat connectivity should increase population spatial synchrony.

While earlier studies using larger raster sizes have shown regional synchrony in precipitation to be the main driver of synchrony in *L. dispar* (Haynes *et al.* 2013, Haynes *et al.* 2018), the results presented here suggest that dispersal may in fact be a prominent driver of synchrony over short distances. The effects of dispersal could have been missed by these earlier studies due to the coarser spatial scale used or because effects of habitat connectivity were not considered. Future studies should seek to consider the effects of both connectivity and synchrony of weather in the same analyses and compare analyses across spatial scales to resolve the discrepancy described here.

In the computation of forest connectivity in Omniscape, there was a channelization effect present especially in the analyses with larger radii (50 km, 100 km) where current being pulled from a larger source area through narrow corridors of forest, such as along certain coastlines, resulted in heightened connectivity values at the narrowest points. However, this probably had little effect on my results because the coastal areas where channelization was most severe (see Fig. 2) generally had little to no defoliation (see Fig. 3).

My approach to examining relationships between population synchrony and habitat connectivity estimated using circuit theory provides a framework for understanding the role of dispersal in driving population spatial synchrony. Many methods have been employed to measure habitat connectivity. Some of these include ‘least-cost’ movement simulations (Adriaensen *et al.* 2003), habitat pattern indices (Schumaker 1996), and models of the movement of individuals through corridors (Hargrove *et al.* 2005). Assessing connectivity based on circuit theory via an iterative moving window is a better alternative because it accounts for all possible movement pathways rather than one ideal or ‘least-cost’ route (McRae *et al.* 2008). In both random-walk models, which can provide useful approximations of dispersal patterns (Schippers *et al.* 1996; Codling *et al.* 2008), and circuit theory, organisms are not assumed to have complete

knowledge of the landscape and thus cannot know an ideal movement pathway (McRae *et al.* 2008). Finally, the existing body of work on circuit theory algorithms promotes their ease of use on large raster grids (McRae *et al.* 2008). Similarly, the ncLISA method used here to map geographic variation in the strength of synchrony is also effective on large raster grids and has been successfully utilized by prior studies to study the drivers of synchrony (Haynes *et al.* 2019; Haynes *et al.* 2013; Gouveia *et al.* 2016).

The approach used here could be applied to a diversity of study systems. Exploration of impacts of different factors known to influence dispersal (e.g., flows of water or wind, habitat connectivity) on population spatial synchrony allows a greater understanding of the importance of dispersal as a driver of synchrony (Castorani *et al.* 2015; Bellamy *et al.* 2003; Anderson *et al.* 2017). Such knowledge can have implications for best practices in pest management. For pest species where dispersal likely contributes to widespread synchronous outbreaks, suppression of localized outbreaks may help prevent a localized outbreak from expanding into a regional-scale outbreak (Johnson *et al.* 2004; Liebhold & McManus 1991; Liebhold *et al.* 2012; Johns *et al.* 2019). In contrast, localized suppression of outbreaks would be unsuccessful at preventing widespread outbreaks in pest species where populations are synchronized by regional-scale environmental fluctuations.

References

Adriaensen, F., Chardon, J. P., De Blust, G., Swinnen, E., Villalba, S., Gulinck, H., & Matthysen, E. (2003). The application of 'least-cost'modelling as a functional landscape model. *Landscape and urban planning*, *64*(4): 233-247.

Aitken, A. C. (1936). IV.—On least squares and linear combination of observations. *Proceedings of the Royal Society of Edinburgh*, *55*: 42-48.

Anantharaman R., Hall K., Shah V., & Edelman A. (2019). Circuitscape in Julia: High performance connectivity modeling to support conservation decisions. Proceedings of JuliaCon. http://arxiv.org/abs/arXiv:1906.03542

Anderson, T. L., Walter, J. A., Levine, T. D., Hendricks, S. P., Johnston, K. L., White, D. S. & Reuman, D. C. (2018), Using geography to infer the importance of dispersal for the synchrony of freshwater plankton. *Oikos*, *127*: 403-414.

Bittner, T. D., Hajek, A. E., Liebhold, A. M., & Thistle, H. (2017). Modification of a pollen trap design to capture airborne conidia of Entomophaga maimaiga and detection of conidia by quantitative PCR. *Applied and Environmental Microbiology*, *83*(17): e00724-17.

Bjørnstad, O. N. (2020). ncf: Spatial Covariance Functions. R package version 1.2-9. https://CRAN.R-project.org/package=ncf

Bjørnstad, O. N., Peltonen, M., Liebhold, A. M., & Baltensweiler, W. (2002). Waves of larch budmoth outbreaks in the European alps. *Science, 298*: 1020–1023.

Bjørnstad, O. N., Stenseth, N. C., & Saitoh, T. (1999). Synchrony and scaling in dynamics of voles and mice in northern Japan. *Ecology, 80*: 622-637.

Brown, J.H., & Kodric-Brown, A. (1977). Turnover rates in insular biogeography: effect of immigration on extinction. *Ecology, 58*: 445-449.

Bullock, J. M., Shea, K., & Skarpaas, O. (2006). Measuring plant dispersal: an introduction to field methods and experimental design. *Plant Ecology*, *186*(2): 217-234.

Castorani, M. C. N., Reed, D. C., Alberto, F., Bell, T. W., Simons, R. D., Cavanaugh, K. C., Siegel, D. A. & Raimondi, P. T. (2015), Connectivity structures local population dynamics: a long-term empirical test in a large metapopulation system. *Ecology, 96*: 3141-3152.

Codling, E. A., Plank, M. J., & Benhamou, S. (2008). Random walk models in biology. *Journal of the Royal society interface*, *5*(25), 813-834.

Cushman, S. A., & McGarigal, K. (2008). Landscape metrics, scales of resolution. In *Designing green landscapes* (pp. 33-51). Springer, Dordrecht.

Daniel, C. (1959). Use of Half-Normal Plots in Interpreting Factorial Two-Level Experiments. *Technometrics*, *1*(4): 311–341.

Dwyer, G., & Elkinton, J. S. (1995). Host dispersal and the spatial spread of insect pathogens. *Ecology, 76*: 1262-1275.

Elkinton, J.S., Bittner, T.D., Pasquarella, V.J., Boettner, G.H., Liebhold, A.M., Gould, J.R., Faubert, H., Tewksbury, L., Broadley, H.J., Havill, N.P. and Hajek, A.E., 2019. Relating aerial deposition of Entomophaga maimaiga conidia (Zoopagomycota: Entomophthorales) to mortality of gypsy moth (Lepidoptera: Erebidae) larvae and nearby defoliation. *Environmental Entomology*, *48*(5): 1214-1222.

Elkinton, J. S., & Liebhold, A. M. (1990). Population dynamics of gypsy moth in North America. *Annual review of entomology, 35*: 571-596.

Fox, J. W., Legault, G., Vasseur, D. A., & Einarson, J. A. (2013). Nonlinear effect of dispersal rate on spatial synchrony of predator-prey cycles. *PloS one*, *8*.

Fox, J. W., Vasseur, D. A., Hausch, S. & Roberts, J. (2011), Phase locking, the Moran effect and distance decay of synchrony: experimental tests in a model system. *Ecology Letters, 14*: 163-168.

Gouveia, A. R., Bjørnstad, O. N., & Tkadlec, E. (2016). Dissecting geographic variation in population synchrony using the common vole in central Europe as a test bed. *Ecology and evolution*, *6*: 212-218.

Hanski, I., & Woiwod, I. P. (1993). Spatial synchrony in the dynamics of moth and aphid populations. *Journal of Animal Ecology, 62*: 656-668.

Hansson, L. (1991). Dispersal and connectivity. In M. Gilpin & I. Hanski (Eds.), *Metapopulation dynamics: empirical and theoretical investigations* (pp. 89-103). Academic Press, London, UK.

Hargrove, W. W., Hoffman, F. M., & Efroymson, R. A. (2005). A practical map-analysis tool for detecting potential dispersal corridors. *Landscape Ecology*, *20*(4): 361-373.

Haynes, K. J., Bjørnstad, O. N., Allstadt, A. J. & Liebhold, A. M. (2013). Geographical variation in the spatial synchrony of a forest-defoliating insect: isolation of environmental and spatial drivers. *Proc. R. Soc. Biol. Sci., 280*.

Haynes, K. J., Liebhold, A. M., Bjørnstad, O. N., Allstadt, A. J., & Morin, R. S. (2018), Geographic variation in forest composition and precipitation predict the synchrony of forest insect outbreaks. *Oikos*, *127*: 634-642.

Haynes, K. J., Liebhold, A. M., Fearer, T. M., Wang, G., Norman, G. W., & Johnson, D. M. (2009), Spatial synchrony propagates through a forest food web via consumer–resource interactions. *Ecology, 90*: 2974-2983.

Haynes, K. J., Liebhold, A. M., Lefcheck, J. S., Morin, R. S., & Wang, G. (2022). Climate affects the outbreaks of a forest defoliator indirectly through its tree hosts. *Oecologia*, *198*: 407-418.

Haynes, K. J., Walter, J. A., & Liebhold, A. M. (2019). Population spatial synchrony enhanced by periodicity and low detuning with environmental forcing. *Proceedings of the Royal Society B*, *286*(1903): 20182828.

Heino, M., Kaitala, V., Ranta, E., & Lindström, J. (1997). Synchronous dynamics and rates of extinction in spatially structured populations. *Proceedings of the Royal Society of London. Series B: Biological Sciences*, *264*: 481-486.

Hesselbarth, M. H. K., Sciaini, M., With, K. A., Wiegand, K., & Nowosad, J. (2019). landscapemetrics: an open-source R tool to calculate landscape metrics. *Ecography 42*: 1648-1657.

Howard, W. E. (1949). Dispersal, amount of inbreeding and longevity in a local population of prairie deer mice on the George Reserve, southern Michigan. *Contrib. Lab. Vertebr. Biol. Univ. Mich.*, *43*: 1-50.

Ims, R. A., & Andreassen, H. P. (2000). Spatial synchronization of vole population dynamics by predatory birds. *Nature*, *408*: 194-196.

Ims, R. A., & Steen, H. (1990). Geographical synchrony in microtine population cycles: a theoretical evaluation of the role of nomadic avian predators. *Oikos*, *57*: 381-387.

Ims, R. A., & Yoccoz, N. G. (1997). Studying transfer processes in metapopulations: emigration, migration, and colonization. In *Metapopulation biology* (pp. 247-265). Academic Press. Johnson, D. M., Liebhold, A. M., & Bjørnstad, O. N.. 2006. Geographical variation in the periodicity of gypsy moth outbreaks. *Ecography*, *29*: 367–374.

Johns, Robert C., Joseph J. Bowden, Drew R. Carleton, Barry J. Cooke, Sara Edwards, Erik JS Emilson, Patrick MA James et al. "A conceptual framework for the spruce budworm early intervention strategy: Can outbreaks be stopped?." *Forests* 10, no. 10 (2019): 910.

Johnson, D. M., Bjørnstad, O. N., & Liebhold, A. M. (2004). Landscape geometry and traveling waves in the larch budmoth. *Ecology Letters*, *7*(10): 967-974.

Johnson, D. M., Liebhold, A. M., Bjørnstad, O. N., & Mcmanus, M. L. (2005). Circumpolar variation in periodicity and synchrony among gypsy moth populations. *Journal of Animal Ecology*, *74*: 882-892.

Koenig, W. D. (2002), Global patterns of environmental synchrony and the Moran effect. *Ecography*, *25*: 283-288.

Krohne, D. T., Dubbs, B. A., & Baccus, R. (1984). An analysis of dispersal in an unmanipulated population of Peromyscus leucopus. *American Midland Naturalist, 112:* 146-156.

Laan, E., & Fox, J. W. (2020). An experimental test of the effects of dispersal and the paradox of enrichment on metapopulation persistence. *Oikos*, *129*: 49-58.

Landau, V.A., V.B. Shah, R. Anantharaman, and K.R. Hall. 2021. Omniscape.jl: Software to compute omnidirectional landscape connectivity. *Journal of Open Source Software, 6*.

Lande, R., Engen, S., & Sæther, B. E. (1999). Spatial scale of population synchrony: Environmental correlation versus dispersal and density regulation. *The American Naturalist*, *154*: 271-281.

Landler, L., Ruxton, G. D., & Malkemper, E. P. (2021). The multivariate analysis of variance as a powerful approach for circular data. Preprint.

Larroque, J., Johns, R., Canape, J., Morin, B., & James, P. M. (2020). Spatial genetic structure at the leading edge of a spruce budworm outbreak: The role of dispersal in outbreak spread. *Forest Ecology and Management*, *461*, 117965.

Larroque, J., Legault, S., Johns, R., Lumley, L., Cusson, M., Renaut, S., ... & James, P. M. (2019). Temporal variation in spatial genetic structure during population outbreaks: Distinguishing among different potential drivers of spatial synchrony. *Evolutionary Applications*, *12*(10), 1931-1945.

Legault, S., Wittische, J., Cusson, M., Brodeur, J., & James, P. M. (2021). Landscape-scale population connectivity in two parasitoid species associated with the spruce budworm: Testing the birdfeeder effect using genetic data. *Molecular Ecology*, *30*(22), 5658-5673.

Liebhold, A. M. *et al.* (1997). *Gypsy moth in the United States, an atlas* (Vol. 233). USDA Forest Service.

Liebhold, A. M., Gottschalk, K. W., Muzika, R., Montgomery, M. E., Young, R., O'Day, K., & Kelley, B. (1995). Suitability of North American Tree Species to the Gypsy Moth: A Summary of Field and Laboratory Tests. General Technical Report NE-211. USDA Forest Service, Randor PA.

Liebhold, A. M., Haynes, K. J., & Bjørnstad, O. N. (2012). Spatial synchrony of insect outbreaks. In Barbosa, P., Letourneau, D. K., & Agrawal, A. A., (Eds). *Insect outbreaks revisited* (pp. 113-125). Blackwell Publishing, Hoboken, NJ.

Liebhold, A., & Kamata, N. (2000). Are population cycles and spatial synchrony a universal characteristic of forest insect populations?. *Population Ecology, 42*.

Liebhold, A., Koenig, W. D. & Bjørnstad, O. N. (2004). Spatial synchrony in population dynamics. *Annual Review of Ecology Evolution and Systematics, 35:* 467–490.

Liehold, A. M., & McManus, M. L. (1991). Does larval dispersal cause the expansion of gypsy moth outbreaks? *Northern Journal of Applied Forestry*, *8*(3): 95-98.

Lindström, J., Ranta, E., & Lindén, H. (1996). Large-scale synchrony in the dynamics of capercaillie, black grouse and hazel grouse populations in Finland. *Oikos, 76*: 221-227.

Maier, T. J. (2002). Long-distance movements by female White-footed Mice, Peromyscus leucopus, in extensive mixed-wood forest. *Canadian Field-Naturalist, 116*: 108-1 1 1

Mason, C. J., & McManus, M. L. (1981). Larval dispersal of the gypsy moth. In *The gypsy moth: research toward integrated pest management* (pp. 161-202).

Matheron, G., (1969). Le Krigeage Universel. *Les Cahiers du Centre de Morphologie Mathématique de Fontainblue, Fascicule 1*.

McFadden, M. W., & McManus, M. E. (1991). An insect out of control? The potential for spread and establishment of the gypsy moth in new forest areas in the United States. In: Baranchikov, Yuri N.; Mattson, William J.; Hain, Fred P.; Payne, Thomas L., (Eds.), *Forest Insect Guilds: Patterns of Interaction with Host Trees* (pp. 172-186). US Department of Agriculture, Forest Service, Northeastern Forest Experiment Station.

McRae, B. H., Dickson, B. G., Keitt, T. H., & Shah, V. B. (2008). Using circuit theory to model connectivity in ecology, evolution, and conservation. *Ecology, 89*: 2712-2724.

Moran, P. A. P. (1953). The statistical analysis of the Canadian Lynx cycle. *Australian Journal of Zoology, 1*: 291-298.

Morin, S. R., & Liebhold, A. M. (2016). Invasive forest defoliator contributes to the impending downward trend of oak dominance in eastern North America. *Forestry, 89*: 284–289.

Morris, D. W., & Diffendorfer, J. E. (2004). Reciprocating dispersal by habitat-selecting white-footed mice. *Oikos, 107*: 549-558.

Munro, V.M.W. (1998). A retrospective analysis of the establishment and dispersal of the introduced Australian parasitoids *Xanthopimpla rhopaloceros* (Krieger) (Hymenoptera: Ichneumonidae) and *Trigonospila brevifacies* (Hardy) (Diptera: Tachinidae) within new Zealand. *Biocontrol Science and Technology, 8*: 559–571.

Nathan, R. (2001). The challenges of studying dispersal. *Trends in Ecology & Evolution*, *16*(9), 481-483.

Oden, N. L., & Sokal, R. R. (1986). Directional autocorrelation: an extension of spatial correlograms to two dimensions. *Systematic Zoology*, *35*: 608-617.

Peltonen, M., Liebhold, A. M., Bjørnstad, O. N. & Williams, D. W. (2002). Spatial synchrony in forest insect outbreaks: Roles of regional stochasticity and dispersal. *Ecology, 83*: 3120-3129.

Pinheiro, J., Bates, D., DebRoy, S., Sarkar, D., & R Core Team (2021). *nlme: Linear and Nonlinear Mixed Effects Models*. R package version 3.1-153, https://CRAN.R-project.org/package=nlme.

Powney, G. D., Broaders, L. K. & Oliver, T. H. (2012). Towards a measure of functional connectivity: local synchrony matches small scale movements in a woodland edge butterfly. *Landscape Ecology, 27*: 1109–1120.

Ranta, E., Veijo, K., & Lindströom, J. (1999). Spatially autocorrelated disturbances and patterns in population synchrony. *Proceedings of the Royal Society of London. Series B: Biological Sciences, 266*: 1851-1856.

Ranta, E., Kaitala, V., Lindström, J., & Linden, H. (1995). Synchrony in population dynamics. *Proceedings of the Royal Society of London. Series B: Biological Sciences, 262*: 113-118.

Ranta, E., Kaitala, V., Lindström, J., & Helle, E. (1997). The Moran effect and synchrony in population dynamics. *Oikos, 78*: 136-142.

Ranta, E., Kaitala, V., & Lundberg, P. (1998). Population variability in space and time: the dynamics of synchronous population fluctuations. *Oikos, 83:* 376-382.

Reardon, R. C., & Podgwaite, J. D. (1976). Disease-parasitoid relationships in natural populations of Lymantria dispar [Lep.: Lymantriidae] in the northeastern United States. *Entomophaga, 21*: 333-341.

Régnière, J., & Bolstad, P. (1994). Statistical simulation of daily air temperature patterns in eastern North America to forecast seasonal events in insect pest management. *Environmental Entomology, 23*: 1368–1380.

Régnière, J., Nealis, V., & Porter, K. (2008). Climate suitability and management of the gypsy moth invasion into Canada. In *Ecological impacts of non-native invertebrates and fungi on terrestrial ecosystems* (pp. 135-148). Springer, Dordrecht.

Régnière, J., & Sharov, A. (1998). Phenology of Lymantria dispar (Lepidoptera: Lymantriidae), male flight and the effect of moth dispersal in heterogeneous landscapes. *International Journal of Biometeorology, 41*: 161-168.

Rieux, A., Soubeyrand, S., Bonnot, F., Klein, E. K., Ngando, J. E., Mehl, A., ... & De Lapeyre de Bellaire, L. (2014). Long-distance wind-dispersal of spores in a fungal plant pathogen: estimation of anisotropic dispersal kernels from an extensive field experiment. *PLoS One, 9*(8), e103225.

Rogers, H. S., Beckman, N. G., Hartig, F., Johnson, J. S., Pufal, G., Shea, K., Zurell, D., Bullock, J. M., Cantrell, R. S., Loiselle, B., Pejchar, L., Razafindratsima, O. H., Sandor, M. E., Schupp, E. W., Strickland, W. C., & Zambrano, J. (2019). The total dispersal kernel: a review and future directions. *AoB Plants, 11*.

Royama, T., MacKinnon, W. E., Kettela, E. G., Carter, N. E., & Hartling, L. K. (2005). Analysis of spruce budworm outbreak cycles in New Brunswick, Canada, since 1952. *Ecology, 86*(5): 1212-1224.

Schippers, P., Verboom, J., Knaapen, J. P., & Van Apeldoorn, R. C. (1996). Dispersal and habitat connectivity in complex heterogeneous landscapes: an analysis with a GIS-based random walk model. *Ecography, 19*(2), 97-106.

Schumaker, N. H. (1996). Using landscape indices to predict habitat connectivity. *Ecology*, 1210-1225.

Sheehan, K. A. (1989). Models for the population dynamics of Lymantria dispar. *General technical report NE-US Department of Agriculture, Forest Service, Northeastern Forest Experiment Station* (pp. 533-547).

Steen, H., Ims, R. A., & Sonerud, G. A. (1996). Spatial and temporal patterns of small-rodent population dynamics at a regional scale. *Ecology, 77*: 2365-2372.

Stenseth, N. C., Chan, K. S., Tong, H., Boonstra, R., Boutin, S., Krebs, C. J., Post, E., O'Donoghue, M., Yoccoz, N. G., Forchhammer, M. C., & Hurrell, J. W. (1999). Common dynamic structure of Canada lynx populations within three climatic regions. *Science, 285*: 1071-1073.

Sutcliffe, O. L., Thomas, C. D., & Moss, D. (1996). Spatial synchrony and asynchrony in butterfly population dynamics. *Journal of Animal Ecology, 65:* 85-95.

Taylor, P. D., Fahrig, L., Henein, K., & Merriam, G. (1993). Connectivity is a vital element of landscape structure. *Oikos, 68:* 571-573.

Tischendorf, L., & Fahrig, L. (2000). On the usage and measurement of landscape connectivity. *Oikos, 90*: 7-19.

Twery, M. J. (1991). Effects of defoliation by gypsy moth. *US Interagency gypsy moth research review, 1584*: 27-39.

USDA Forest Service. (2018). Individual Tree Species Parameter Maps. USDA Forest Service. https://data.nal.usda.gov/dataset/individual-tree-species-parameter-maps.

Vindstad, O. P. L., Jepsen, J. U., Yoccoz, N. G., Bjørnstad, O. N., Mesquita, M. D. S., & Ims, R. A. (2019). Spatial synchrony in sub-arctic geometrid moth outbreaks reflects dispersal in larval and adult life cycle stages. *Journal of Animal Ecology, 88*: 1134-1145.

Vogwill, T., Fenton, A. & Brockhurst, M. A. (2009), Dispersal and natural enemies interact to drive spatial synchrony and decrease stability in patchy populations. *Ecology Letters, 12*: 1194-1200.

Walter, J. A., Sheppard, L. W., Anderson, T. L., Kastens, J. H., Bjørnstad, O. N., Liebhold, A. M. & Reuman, D. C. (2017). The geography of spatial synchrony. *Ecology Letters, 20*: 801-814.

Weseloh, R. M. (2003). Short and long range dispersal in the gypsy moth (Lepidoptera: Lymantriidae) fungal pathogen, Entomophaga maimaiga (Zygomycetes: Entomophthorales). *Environmental Entomology, 32*: 111-122.

Williams, D. W., & Liebhold, A. M. (1995). Forest defoliators and climatic change: potential changes in spatial distribution of outbreaks of western spruce budworm (Lepidoptera: Tortricidae) and gypsy moth (Lepidoptera: Lymantriidae). *Environmental entomology, 24*: 1-9.

Wilson, B. T., Lister, A. J., & Riemann, R. I. (2012). A nearest-neighbor imputation approach to mapping tree species over large areas using forest inventory plots and moderate resolution raster data. *Forest ecology and management, 271*: 182-198.

Wilson, B. T., Lister, A. J., Riemann, R. I., & Griffith, D. M. (2013). Live tree species basal area of the contiguous United States (2000-2009). Newtown Square, PA: USDA Forest Service, Rocky Mountain Research Station. https://doi.org/10.2737/RDS-2013-0013

Ydenberg, R. C. (1987). Nomadic predators and geographical synchrony in microtine population cycles. *Oikos, 50:* 270-272.

Appendix

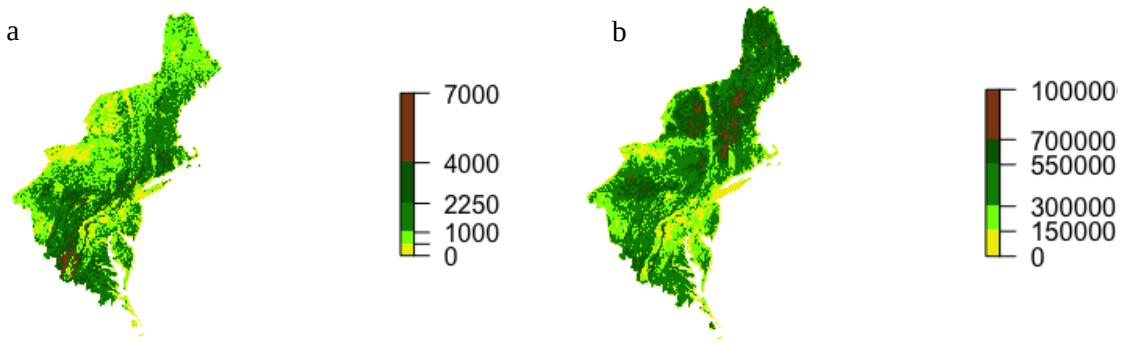

Figure A1.1. Maps at 4km resolution of basal area (m^2/km^2) of *Lymantria dispar* host trees (a) and basal area of all tree species combined (b), ranging from low (yellow) to high (brown), from the Individual Tree Species Parameter Maps (Wilson *et al.* 2013). The extent of the map is limited to the areas of the U.S. infested with *L. dispar* by 1990 (excluding Michigan).

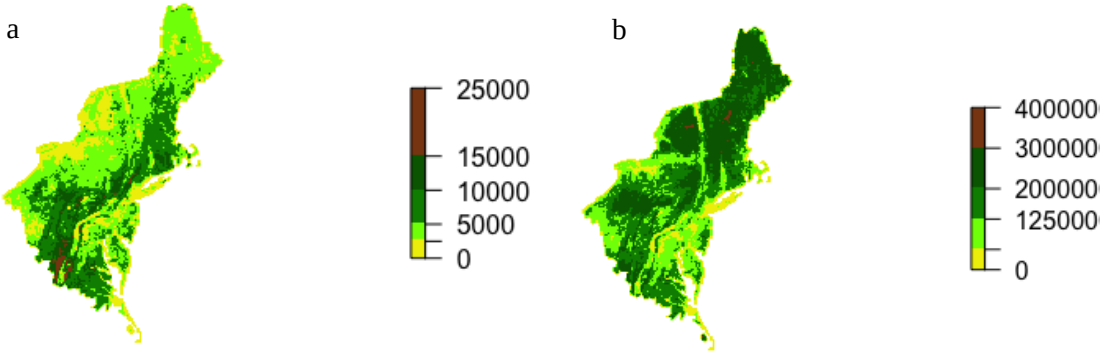

Figure A1.2. Maps at 8km resolution of basal area (m^2/km^2) of *Lymantria dispar* host trees (a) and basal area of all tree species combined (b), ranging from low (yellow) to high (brown), from the Individual Tree Species Parameter Maps (Wilson *et al.* 2013). The extent of the map is limited to the areas of the U.S. infested with *L. dispar* by 1990 (excluding Michigan).

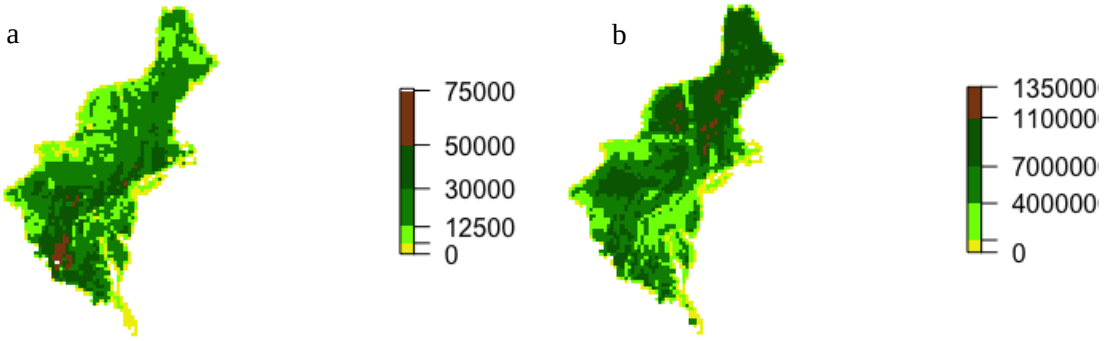

Figure A1.3. Maps at 16km resolution of basal area (m^2/km^2) of *Lymantria dispar* host trees (a) and basal area of all tree species combined (b), ranging from low (yellow) to high (brown), from the Individual Tree Species Parameter Maps (Wilson *et al.* 2013). The extent of the map is limited to the areas of the U.S. infested with *L. dispar* by 1990 (excluding Michigan).

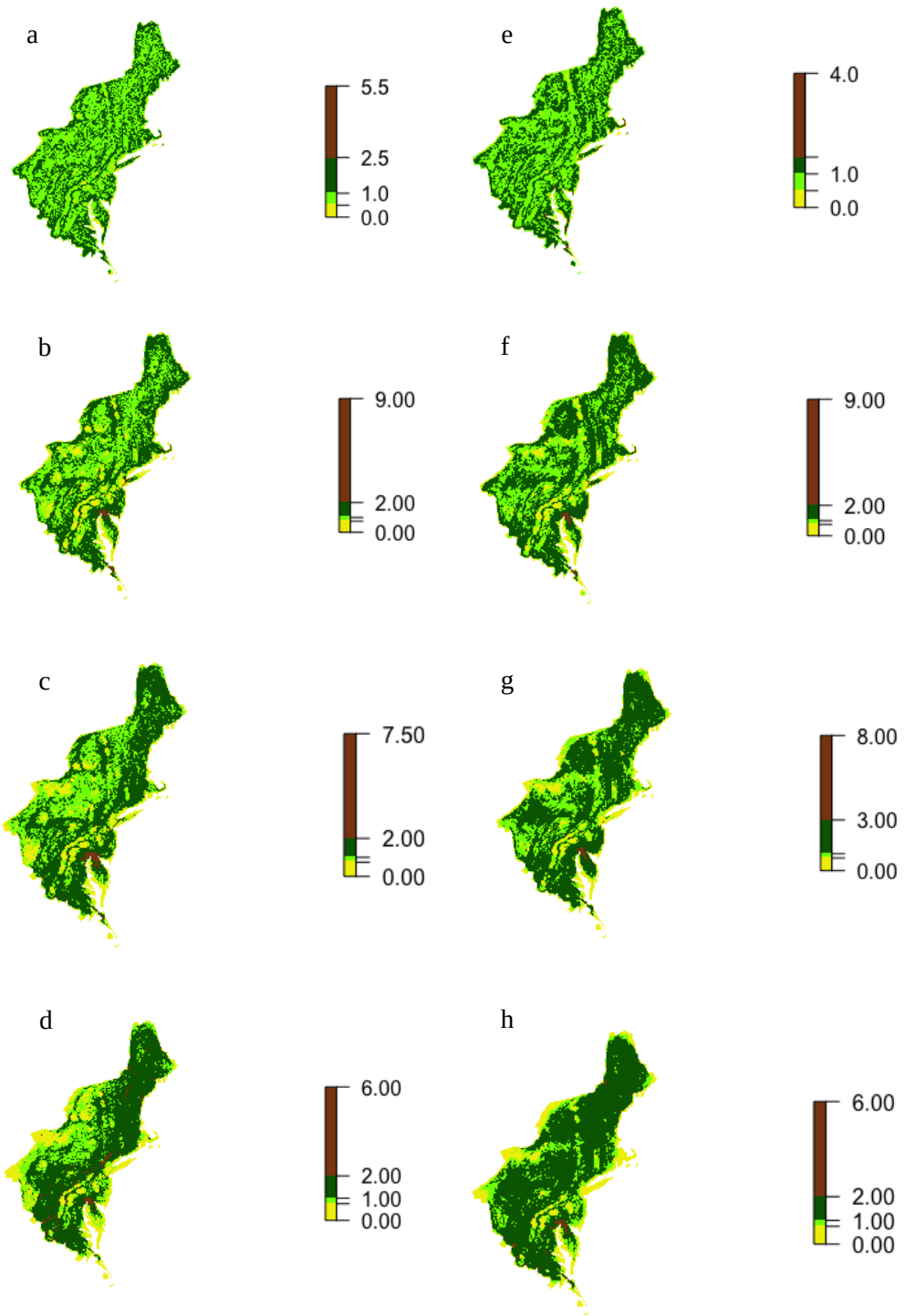

Figure A2.1. Maps of normalized cumulative current (NCC) where the conductance of 16-km^2 cells was the basal area of *Lymantria dispar* host trees (left column, a-d) or the basal area of all tree species combined (right column, e-h). The NCC flowing to each focal cell from all cells within a neighborhood of a given size (within 10km, 25km, 50km, and 100km respectively) are shown. Values of NCC less than one indicate impeded connectivity, while values greater than one indicate channelized flow.

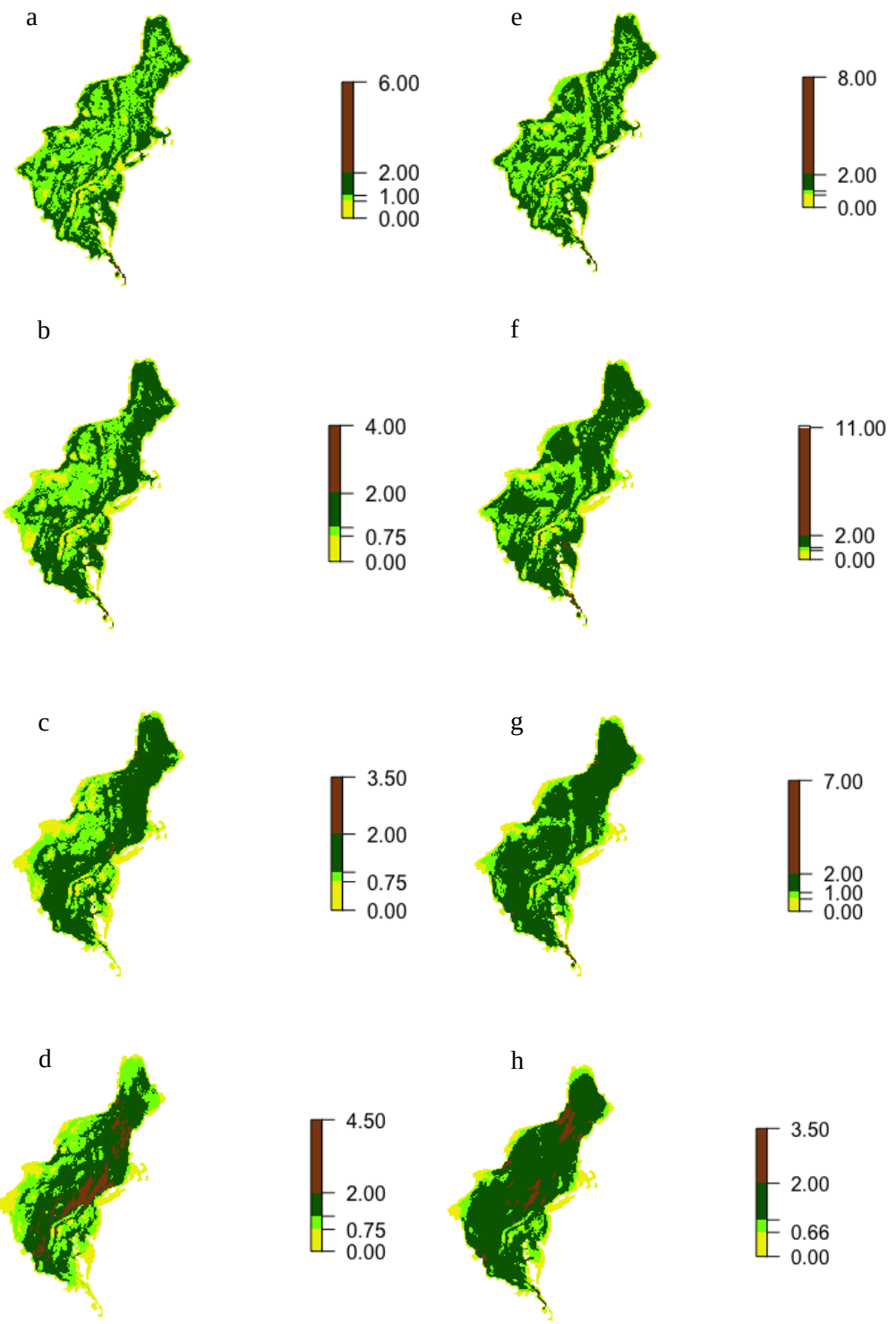

Figure A2.2. Maps of normalized cumulative current (NCC) where the conductance of 64-km^2 cells was the basal area of *Lymantria dispar* host trees (left column, a-d) or the basal area of all tree species combined (right column, e-h). The NCC flowing to each focal cell from all cells within a neighborhood of a given size (within 10km, 25km, 50km, and 100km respectively) are shown. Values of NCC less than one indicate impeded connectivity, while values greater than one indicate channelized flow.

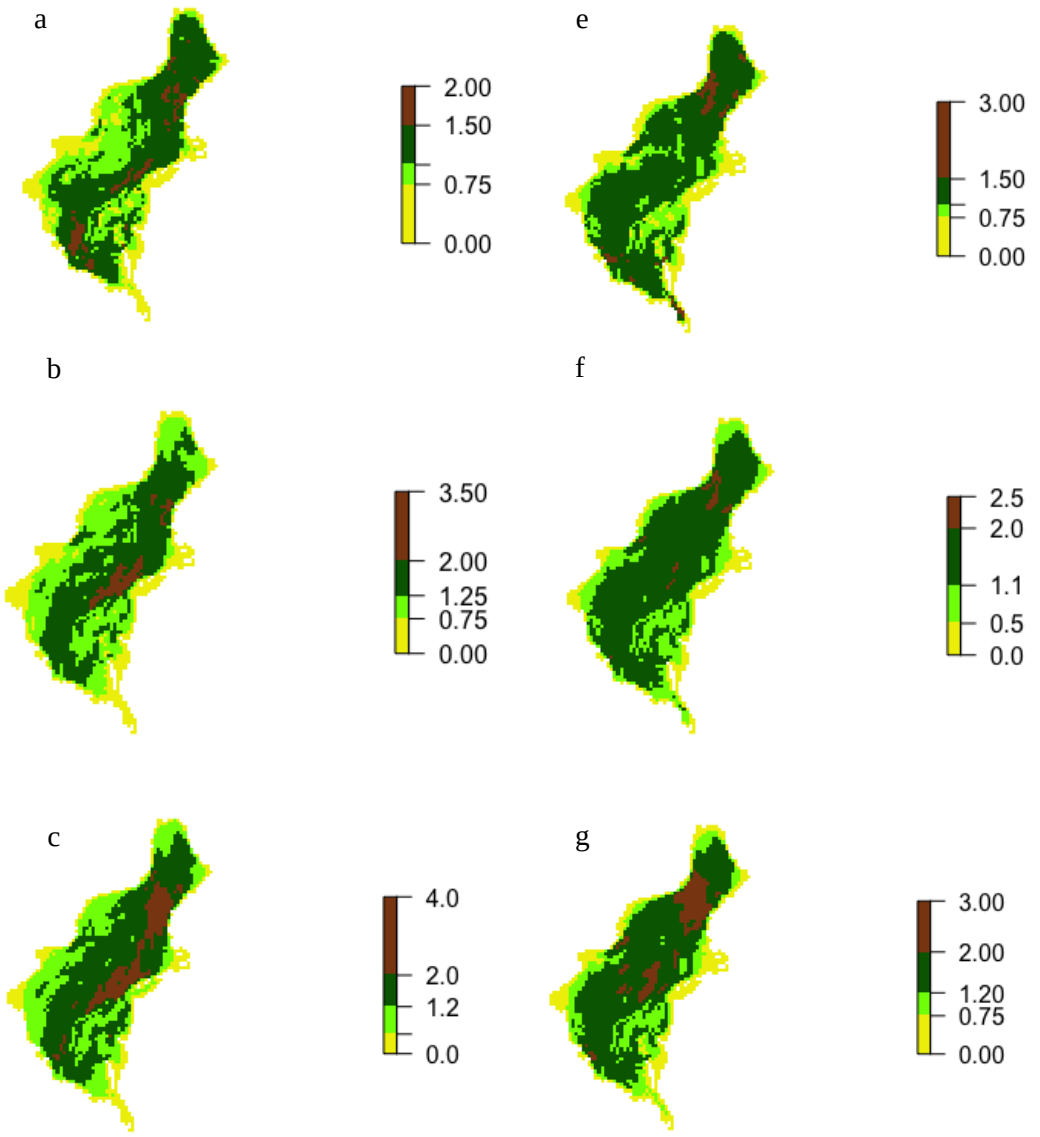

Figure A2.3. Maps of normalized cumulative current (NCC) where the conductance of 256-km^2 cells was the basal area of *Lymantria dispar* host trees (left column, a-c) or the basal area of all tree species combined (right column, e-g). The NCC flowing to each focal cell from all cells within a neighborhood of a given size (within 25km, 50km, and 100km respectively) are shown. Values of NCC less than one indicate impeded connectivity, while values greater than one indicate channelized flow.

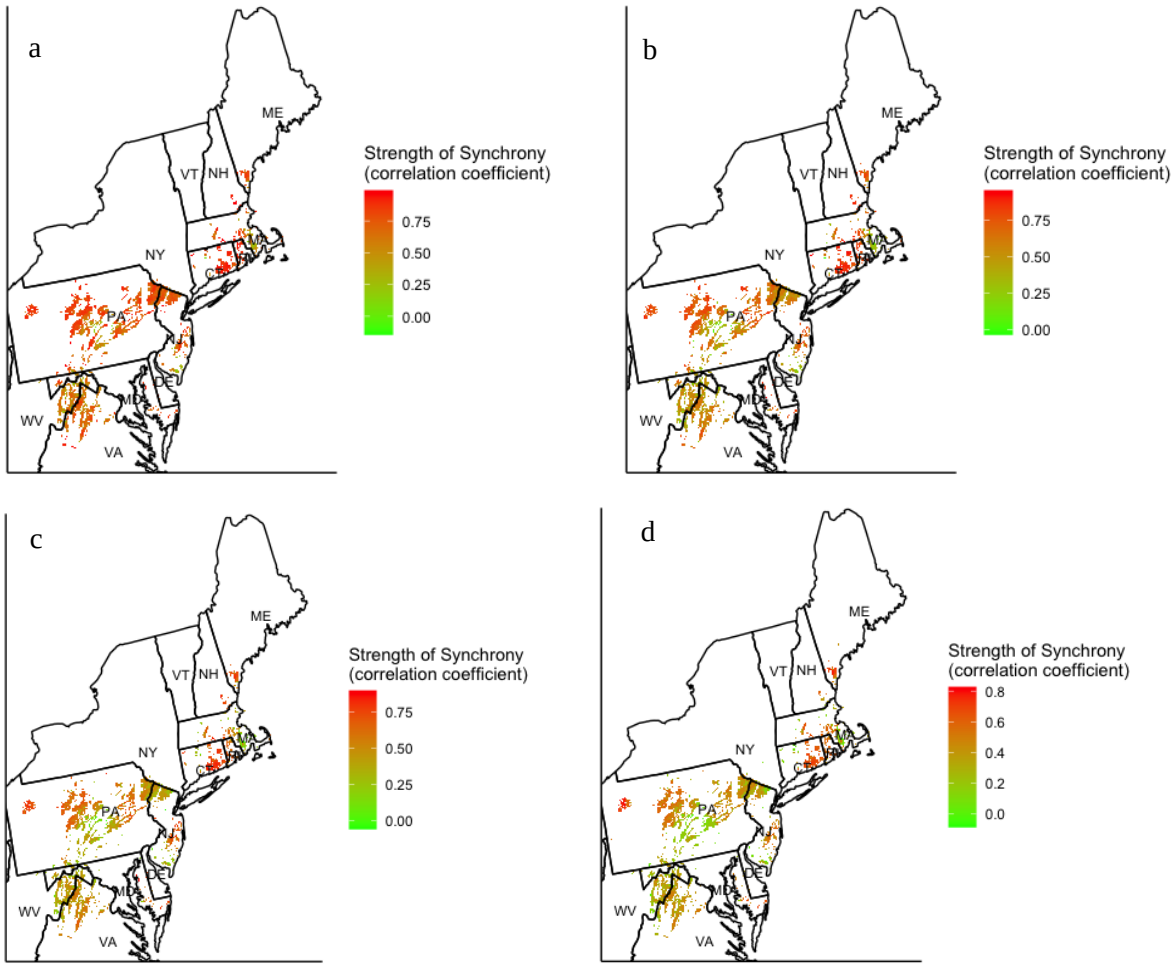

Figure A3.1. Maps at 4km resolution of strength of synchrony in defoliation by *Lymantria dispar* for all cells with four or more years of defoliation. The strength of local synchrony in defoliation for each of these focal cells was calculated using the non-centered local indicator of spatial association (ncLISA; Gouveia *et al.* 2016) and estimated as the mean of the pairwise measures of synchrony (Pearson correlation) in defoliation between the focal cell and all surrounding cells within a neighborhood of specified size (within a radius of 10km, 25km, 50km, and 100km respectively, a-d).

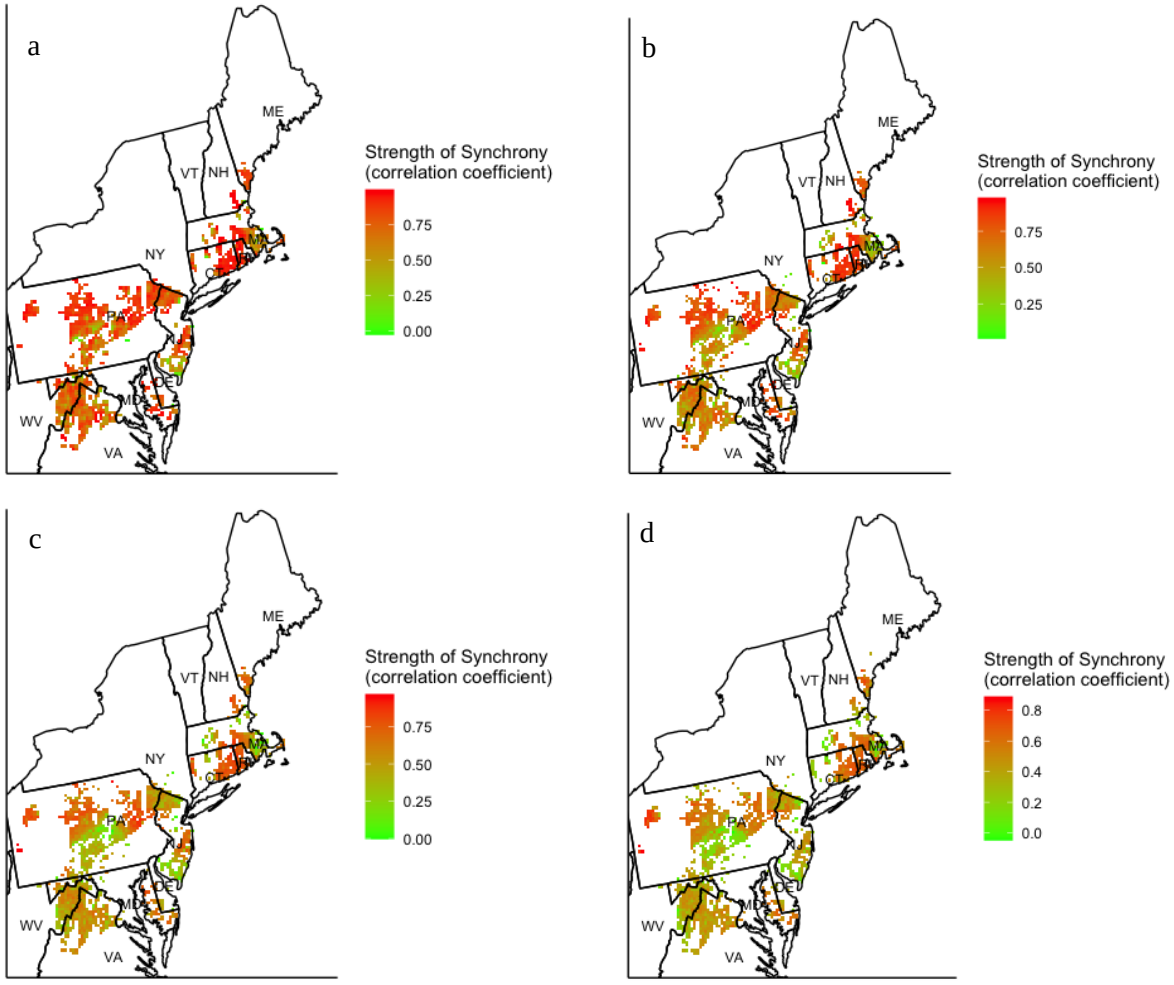

Figure A3.2. Maps at 8km resolution of strength of synchrony in defoliation by *Lymantria dispar* for all cells with four or more years of defoliation. The strength of local synchrony in defoliation for each of these focal cells was calculated using the non-centered local indicator of spatial association (ncLISA; Gouveia *et al.* 2016) and estimated as the mean of the pairwise measures of synchrony (Pearson correlation) in defoliation between the focal cell and all surrounding cells within a neighborhood of specified size (within a radius of 10km, 25km, 50km, and 100km respectively, a-d).

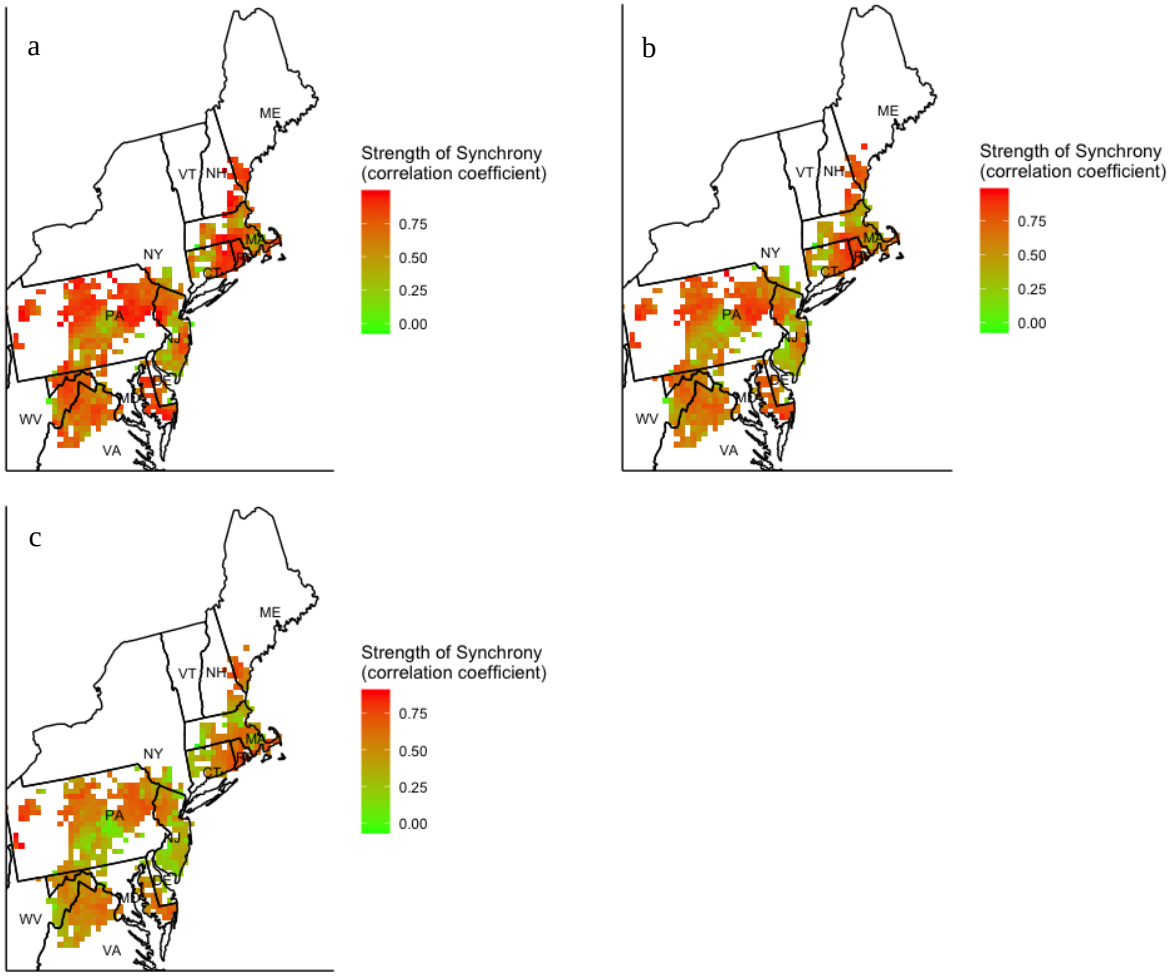

Figure A3.3. Maps at 16km resolution of strength of synchrony in defoliation by *Lymantria dispar* for all cells with four or more years of defoliation. The strength of local synchrony in defoliation for each of these focal cells was calculated using the non-centered local indicator of spatial association (ncLISA; Gouveia *et al.* 2016) and estimated as the mean of the pairwise measures of synchrony (Pearson correlation) in defoliation between the focal cell and all surrounding cells within a neighborhood of specified size (within a radius of 25km, 50km, and 100km respectively, a-c).

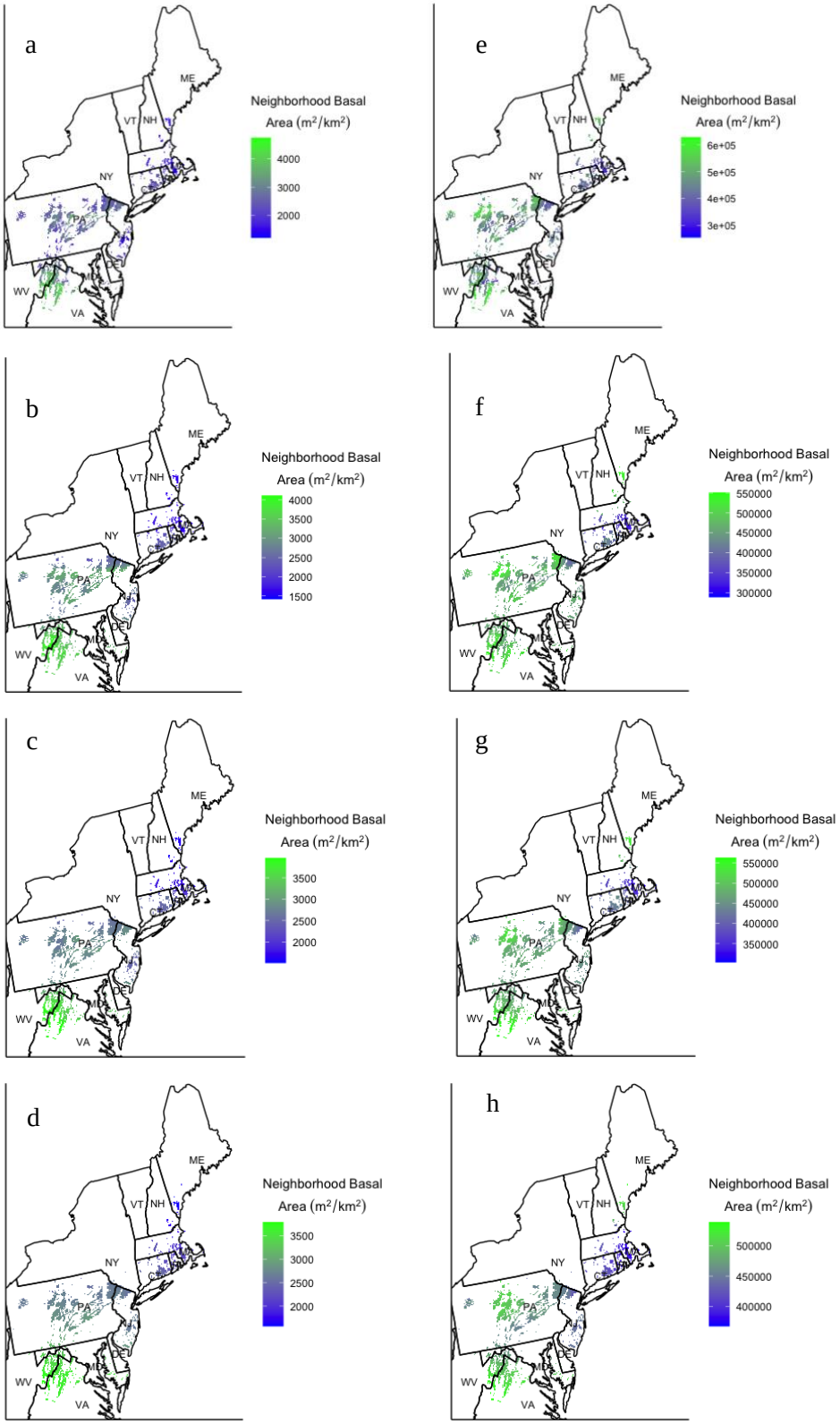

Figure A4.1. Maps at 4km resolution of mean neighborhood basal area of the basal area of *Lymantria dispar* host trees (left column, a-d) or the basal area of all tree species combined (right column, e-h). The means calculated within a neighborhood of a given size (within 10km, 25km, 50km, and 100km respectively) are shown.

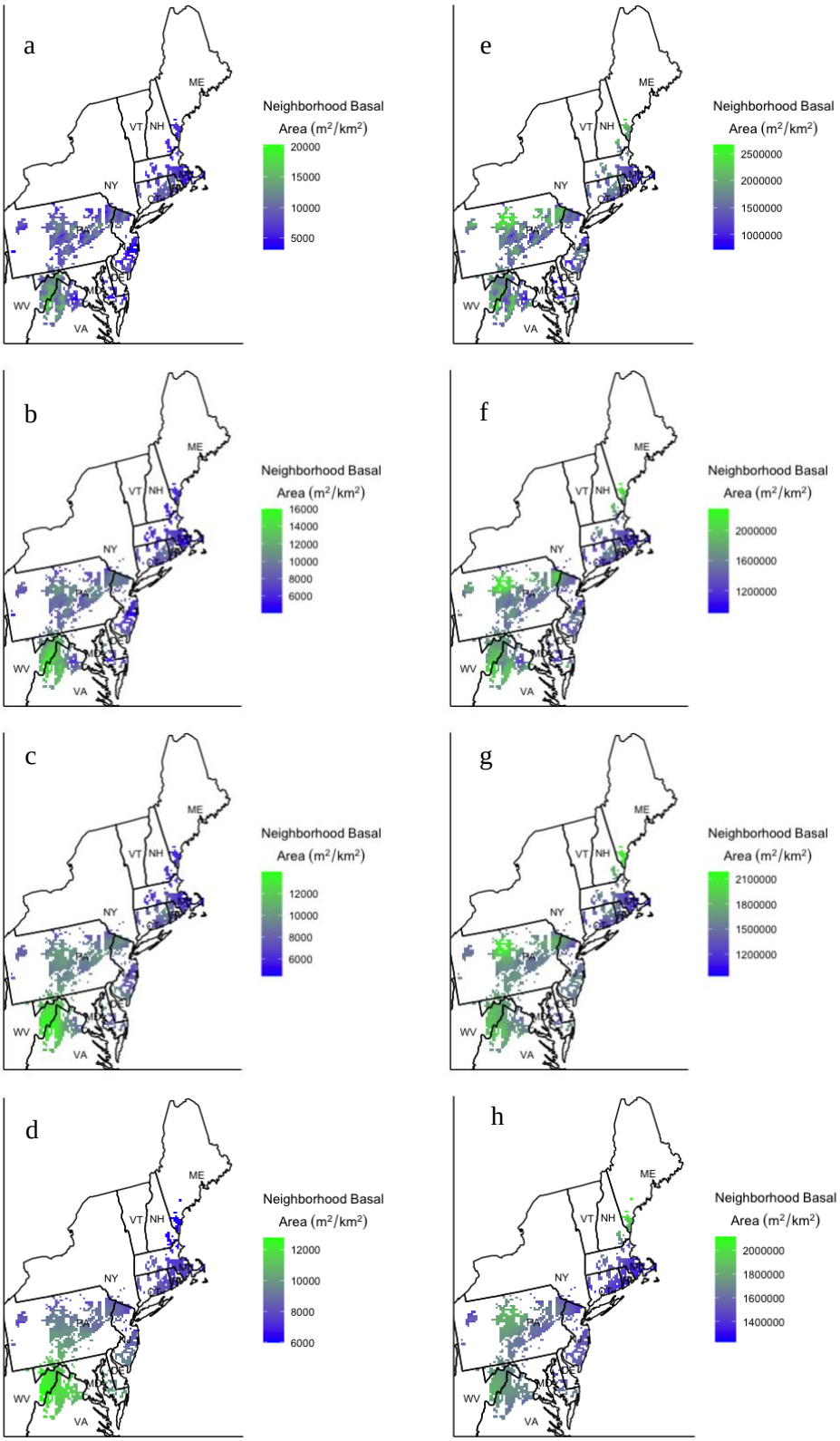

Figure A4.2. Maps at 8km resolution of mean neighborhood basal area of the basal area of *Lymantria dispar* host trees (left column, a-d) or the basal area of all tree species combined (right column, e-h). The means calculated within a neighborhood of a given size (within 10km, 25km, 50km, and 100km respectively) are shown.

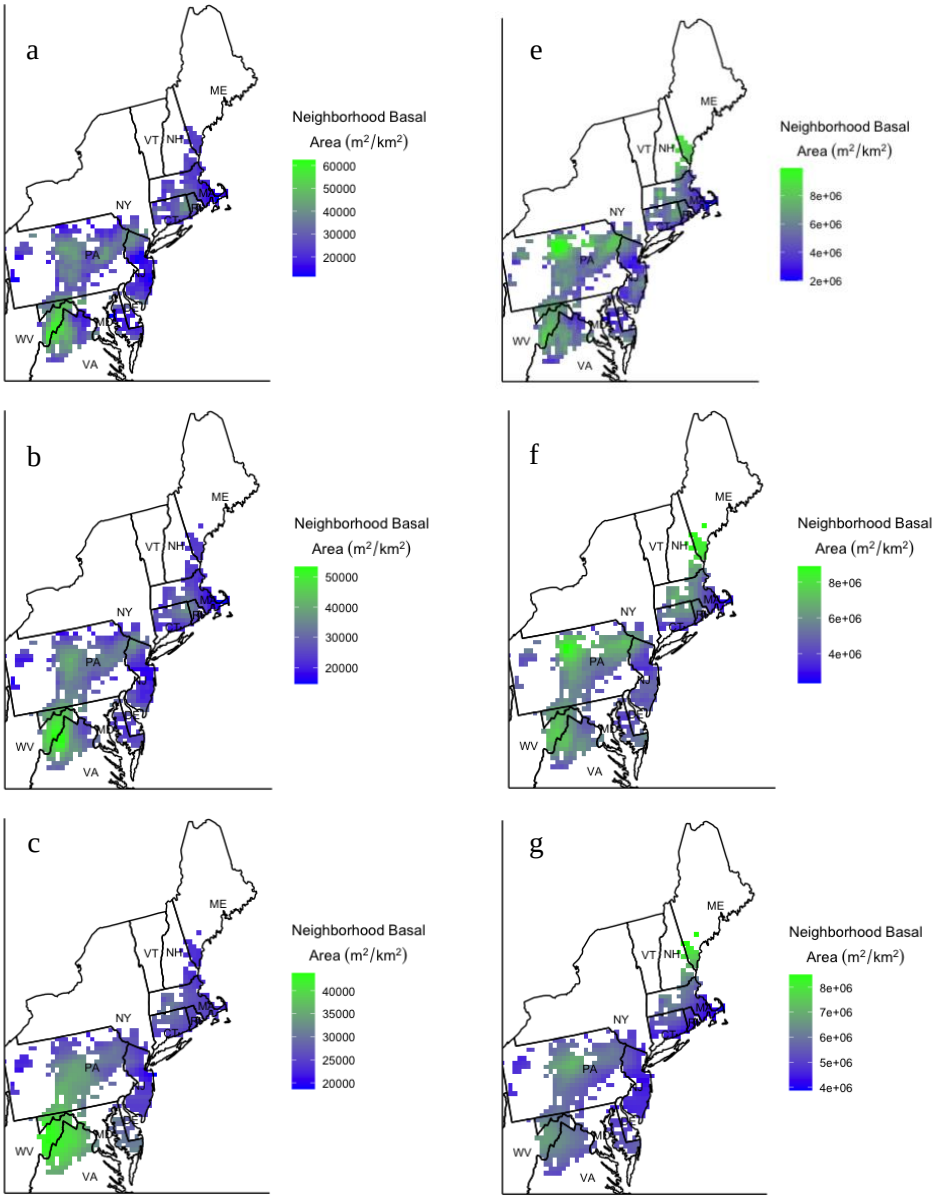

Figure A4.3. Maps at 16km resolution of mean neighborhood basal area of the basal area of *Lymantria dispar* host trees (left column, a-c) or the basal area of all tree species combined (right column, e-g). The means calculated within a neighborhood of a given size (within 25km, 50km, and 100km respectively) are shown.